On Fine Structure in Solar Flares from SDO, RHESSI and TRACE Observations

G. A. Porfir'eva and G. V. Yakunina

Moscow State University, Sternberg Astronomical Institute, Moscow, Russia,

E-mail: yakunina@sai.msu.ru

Abstract. Data on white-light flares (WLFs) on the Sun have been collected. Results of observations in Hα, UV, near infra-red (NIR), X-ray and white-light (WL) on the ground and aboard SDO, RHESSI, Hinode, TRACE SOHO and STEREO are analyzed. Characteristics of flares and relation between continuum emission and Hard X-rays (HXRs) are considered. Usually WL and HXR origin in the footpoints of flaring loops in lower dense layers of the solar atmosphere; however, if the loop density is high enough, WL, HXR and radio emission can originate in the flaring arch itself. Continuum enhancement varies in a wide range. The problem of the heights, where the WL and HXR are formed, is discussed. Observational and theoretical aspects are considered.

Introduction

Solar flares are observed at a broad spectral range and they are often geoeffective. Images, obtained simultaneously in optical, UV, EUV, and X-rays, demonstrate complexity and variability of flare structures. The flare bulk extends from the uppermost photosphere throughout the chromosphere and transition region up to low corona. High energetic electrons, accelerated in the corona, penetrate into lower solar atmosphere producing HXR emission in flaring loop footpoints while low energetic electrons producing SXR emission do not penetrate deeply. However, it is not known where flare continuum emission originates.

For the first time, a WLF, with a visible continuum emission enhancement, was observed in the nineteenth century (Carrington flare). The white-light flares (WLFs) were previously believed to be associated with the most energetic events. Later, an enhanced continuum emission has been revealed in weak C-class flares, while some strong events do not demonstrate enhancement of continuum and in UV and IR range. The weak WLFs C2.7 on 2002 July 25 and C1.6 on 2004 July 24 are discussed by Hudson et al. (2006) and Fletcher et al. (2007). Continuum flare emission is purely investigated up to now. The most WLFs show distinct Balmer and Pashen jumps in their continuum emission that might be explained   due to hydrogen recombination in the chromosphere. For the WLFs, not demonstrating continuum jumps, the usual emission of negative hydrogen ions is important. In reality both these processes act.   The heights, at which the continuum enhancement is produced, can range from the photosphere to lower chromosphere. Results of spatially and temporally resolved observations of solar flares obtained during last decades have been collected to consider morphological and physical characteristics of flares. Analysis of flare properties help to understand better processes of flare origin and development.

Data

To analyze WLFs we used information from published scientific papers and Internet. Additional data containing animated images of the limb WLF M3.5 on 2011 February 24 is available at http://www.astro.gla.ac.uk/users/mbattaglia/20110224_online_material/. For some events simultaneous images at EUV, X-rays and flare continuum are compared.

Results and discussion

Observations in visible spectral region on the ground and UV and EUV from the space show fine structures in flare ribbons and coronal loops. Doschek et al. (1995) found uncorrelated intensity variations in adjacent pixels of an image of a SXR flare loop, which appeared a single one, and suggested that there were flare structures below the resolution capability of the SXT Yohkoh. Line profiles demonstrate complex shapes being a response to complexity and dynamic variability of the solar transition region and coronal active structures (Delone et al., 2003). Observations with TRACE have shown that plasma in solar flares is not confined to a single loop or a few ones. It is clearly demonstrated by Warren (2000) who investigated 4 large two-ribbons flares with long durations. Rising arcades composed from loops were seen, and multiple fine distinct structures were visible with diffused clouds around the arcades. SXT *Yohkoh* flare images look diffuse. Although the peak hotter loops are observed as diffuse it appears more real that both the flare peak and decaying phase plasma are confined in fine structure. Fine structures are distinctly visible on the Figure 1 where a TRACE 19.5 nm image of the flare on 2002 April 21 is presented. Bright loop arcade is seen in a diffused shell of hot plasma. Spatially and temporally resolved observations of flares on SDO and

RHESSI confirm TRACE results (Cheng et al., 2011; Reeves and Golub, 2011; Lemen et al., 2012).
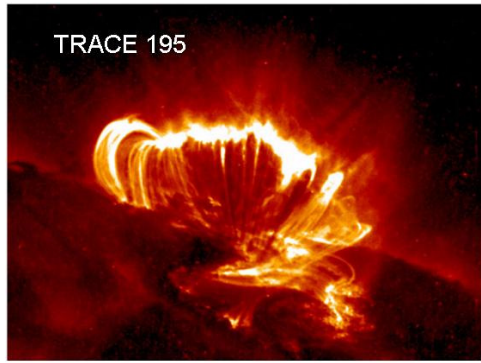
Fig. 1. Bright 2 MK TRACE EUV loops and diffused hot 15 MK current sheet above the loops in the flare on 2002 April 21.
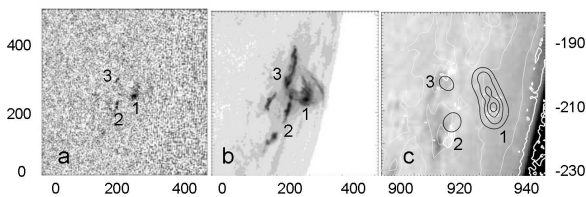
Fig.2. The WLF C9.9 observed on TRACE and RHESSI on 2002 November 12 in WL (a), 170 nm (b), and in HXR (c).
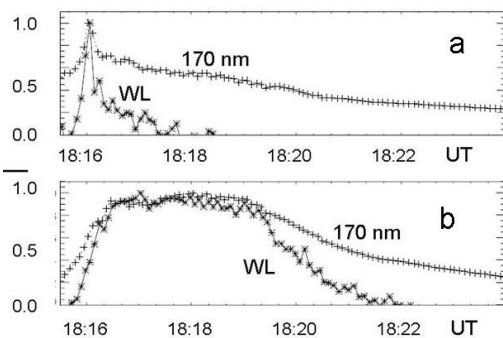
Fig. 3. Emission normalized to its maximum in loop footpoint (a) and top (b) for the WLF C9.9 on 2002 November 12.

Besides the flares of Masuda–type, HXR and white-light (WL) emission is observed in the denser solar atmosphere layers at the loop footpoints. But for dense corona HXR and WL can originate in the loop legs and top. Such events are rare. Images of such flares are shown in Figure 2 where the WLF C9.9 observed on 2002 November 12 is shown in WL (a), 17.0 nm (b), by Fig. 7 from Hudson et al. (2006), and in HXR (c), by Fig. 5 from Fletcher et al. (2007). In Figure 2 (a, b) images scales are in TRACE pixels and in others in arc seconds. The WL emission is seen to extend in the loops themselves. The brightest patches are indicated by the figures. The light curves for one flare loop foot point (a), and for loop top (b) for this WLF is presented in Figure 3. Also flares when looking in radio waves as loops are usually not observed but dense arches can be seen in radio. In Figure 4 the limb flare X3.1 of 2002 August 24 is

presented as observed in HXR on RHESSI (a), in 19.5 nm on TRACE (b), and in radio waves on Norikura Radio Heliograph NoRH (c), by Figure 7 from White et al. (2011). Contours in 17 GHz are imposed on the flare image in 34 GHz (color versions of the figures see in the electronic edition).

The two-ribbon WLF X6.5 on 2006 December 6 is analyzed by Krucker et al. (2011) using the observations on Hinode and RHESSI. Images in continuum near G-band (spectral range $\Delta\lambda$=0.8 nm) at a spatial resolution of 0.18"/px show narrow flare ribbons with the width changing along the ribbon length from 0.5" to 1.8" only. Fine structure of ribbons was distinctly visible in continuum around 430.5 nm and around 160 nm (see Fig. 2 from Krucker et al., 2011). The HXR primary source seems to be even less than 1.1". The location of the flare on the solar disc (S06, E63) does not give a possibility to evaluate heights of the origin of WL and HXR emission.

WL emission is typically seen broken up into small patches within the flare ribbons observed more distinctly in UV. For the WLF 4B/X3.4 on 2006 December 13, observed on Hinode, flare ribbons were well seen in the Ca II 397 nm line, and small kernels were seen on the difference images in the continuum near G-band. The G band kernels coincide spatially with the sites of maximum of both magnetic reconnection rate and energy release along the flare ribbons (Jing et al., 2008). In (Xu et al., 2006) two two-ribbon WLFs on 2003 October 29 (X10, S17, W10) and November 2 (X8, S17, W63) were analyzed using observations at 1.56 μm ($\Delta\lambda$=5 nm, a cadence of 2 s), G-band ($\Delta\lambda$=0.5 nm, a cadence of 2 s) and 520 nm ($\Delta\lambda$=52 nm, a cadence of 1 minute) with 0.1-0.07"/px at the NSO (National Solar Observatory) at Sacramento Peak. Difference images show fine structures. The flare kernel consists of a bright inner part and a weaker outer halo. Xu et al. (2004) demonstrated that NIR flare kernels were located along HXR flare ribbons.

WLFs and HXRs are known to be associated by time and location on the solar disc. Modern observations give new possibilities. The observed correlation suggests that electron acceleration and WLFs are closely related. Watanabe et al. (2010) considered the WLF X1.5 on 2006 December 14 using the observations at G-band (Hinode/SOT) and X-ray (RHESSI). Images at G-band were taken every 2 minutes with a resolution of 0.109"/px and exposure of 0.031s. Two footpoints with a complex fine structure were seen. The south foot point was observed in WL, 20-30 keV and 40-100 keV. The coincidence of WL and 40-100 keV centers were very well. The north foot point has a complex splitting structure. The 20-30 keV emission was separated 8-10" to the south from the site of the WL and 40-100 keV emissions. The WL north foot point location correlates with the HXR one. The exact height of the emission is not determined. Difference between the heights of the WL and HXR emission might be less than usually supposed (Watanabe et al., 2010).

As it is known intensities of WLFs and HXR emission are related. For the WLF X1.5 on 2006 December 14

the G-band and HXR intensities at 40 - 100 keV are well correlated (Figure 5, by Fig. 1 from Watanabe et al., 2010). Correlations between emissions in 1.56 μm and HXR for the flares X10 on 2003 October 29 and X8 on 2003 November 2 are shown by Xu et al. (2006). The time lag between HXR and continuum emission in 1.56 μm is of 20-30 s, that agrees with the time of photosphere heating. However, the opacity during the flare must change and therefore the 1.56 μm continuum might originate higher in photosphere and chromosphere.

WLF continuum emission excess related to the photospheric background defines the contrast

$$c=100(I_{fl}-I_{ph})/I_{ph}$$

that can vary from several to 100 and more %. WLF continuum emission peak is displaced in UV spectral region. Thus the contrast in UV is greater than in visible λλ, and the effective temperature T_{eff} is about 10^4 K (Kretzschmar, 2011). Data on continuum contrast c are collected by us and presented in Table 1. The TRACE WL channel has also some sensitivity to the UV, and therefore WL contrasts include some information about the UV emission and values are overstated in comparison with ground-based observations. In Table 1 the values c are given without correction. Ding (2007) simulated flaring solar atmosphere suggesting heating of the chromosphere by accelerated electrons and temperature minimum region and photosphere by back warming. He received that more energetic emission originates in lower atmosphere and the continuum contrast increases when electron energy increases, and is larger in visible than in NIR λλ and for the limb flares.

Heights of the origin of WLFs and HXR emission are associated. However, it is not clear where WL continuum is originated as comparing with HXR flare emission. Besides the difficulties due to projection effects there are difficulties of alignments of different images from different instrument and insufficient temporal and space resolution. Satisfying models of the flaring solar atmosphere are absent. Limb flares, being more suitable for studying, do not occur often. The limb WLF M3.5 on 2011 February 24 observed in EUV and visible continuum (617.3 nm) from SDO and in X-ray from RHESSI was analyzed by Battaglia and Kontar (2011a) and some later by Oliveros et al. (2012). The flare was associated with the filament eruption (Figure 6, by Fig. 2 from Battaglia and Kontar, 2011a). The coronal SXR source above the solar limb (red) and two HXR footpoints (blue) were seen. Different loops and patches are visible in various λλ. It has been found that 35-100 keV HXR sources were located at heights of 0.8 – 1.7 Mm above the photosphere, the 617.3 nm originated at 1.5 – 3 Mm, maximal EUV emission was observed at height of about 3 Mm and SXR emission was located at the loop top in corona. The EUV emission was produced by low energy electrons of ~12 keV at the top of chromosphere or low corona, where fully ionized matter exists. The WL continuum appeared in the transition layers with densities of 10^{11} cm^{-3} - 10^{13} cm^{-3} between ionized and neutral matter. The HXR

footpoints were observed in lower neutral chromosphere produced by electrons with energies greater than 20 keV. The heights were determined using the method described by Battaglia and Kontar (2011b) and thick target fit to the spatially 5" – 10" integrated spectrum.
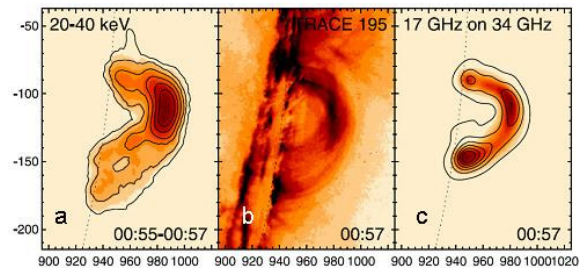
Fig. 4. The limb flare X3.1 on 2002 August 24 in RHESSI HXR (a), TRACE 19.5 nm (b) and NorRH radio waves (c).
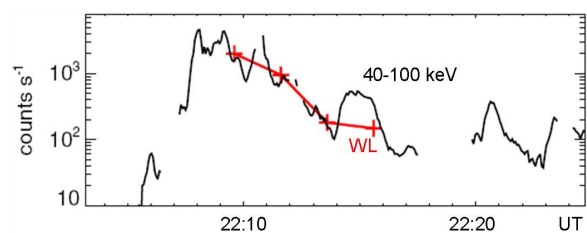
Fig. 5. The WLF X1.5 on 2006 December 14. The continuum intensities in G-band and HXR emission are well correlated.
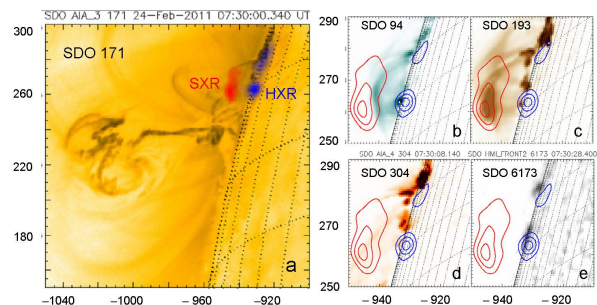
Fig. 6 The limb WLF M3.5 on 2011 February 24, associated with a filament eruption, at 07:30 UT: RHESSI SXR and HXR emission superimposed on SDO 17.1 nm image (a); SDO EUV difference images at 9.4 nm (b), 19.3 nm (b), 30.4 nm (c), and WL (617.3 nm) continuum (d) with X-ray contours overlaid.

Oliveros et al. (2012), using addition observations in 19.5 nm from STEREO B, confirmed that the limb WLF on 2011 February 24 really occurred on the visible side of the solar disc, being observed from the Earth. They evaluated the heights of the HXR emission as 305 ± 170 km and WL emission as 195 ± 70 km. The heights seem to be understated. Oliveros et al. (2012) believe that further observations and investigations are necessary.

Accordingly observations and theoretical simulations HXR sources with higher energy have smaller vertical and horizontal sizes and locate at lower heights above the photosphere than sources with weaker energy because the energetic electrons penetrate in deeper chromospheric layers.

Kontar et al. (2010) found the relation between dimension and height of the HXR source and its energy for the limb flare M5.8 on 2004 January 6. They also simulated such relations using a thick target model and homogenous and multi component chromosphere models. The source dimension does not depend on the model, and observed relation between source dimension and its energy agrees better with the multi component solar chromosphere. For the WLF X1.5 on 2006 December 6 the continuum emission in G-band was found to be at 0-100 km and (50–100) keV HXR at ~6500 km (Watanabe, et al., 2010). Battaglia and Kontar (2011b) using a thick target model evaluated that HXR emission with the energies between 120 keV and 25 keV are formed at the heights between 600 and 1200 km.

Table 1. Continuum contrast C in WLFs

Date	Class	Location	λ	Observatory	C,%	Reference
10.03 2001	M6.7	N27W42	854.2 nm	STT Nanjing	3-5	Liu, Ding, Fang (2001)
25.07.2002	C2.7	S13E46	WL	TRACE	10	Hudson et al. (2006)
26.07.2002	M1.0	S21E21			155	
4.10.2002	M4.0	S19W09			158	
5.10.2002	M1.2	S20W24			56	
12.11.2002	C9.9	S11W75			23	
12.06.2003	M7.3	N13W65			197	
23.10.2003	M2.4	N03E15			339	
29.10.2003	X10	S17W10	1.56μ	Sacramento	18-25	Xu et al. (2004, 2006)
			520nm	Peak	45	
			G-band		75	
2.11.2003	X8	S17W63	1.56μ		66	
			520nm		76	
			G-band		230	
9.01.2004	M3.2	N02E49	WL	TRACE	178	Hudson et al. (2006)
22.07.2004	M9.1	N12W03			414	
24.07.2004	C1.6	N12W03			8	
24.07.2004	C4.8	N04W16			146	
4.06.2007	M8.7		Blue cont.	Hinode	94	Wang (2009)
			G-band		175	
24.08.2007	C2.0	S05E33	395.4nm	SST La Palma	300	Jess et al. (2008)
12.06.2010	M2.0	N22W45	617.3nm	HMI SDO	>10	Oliveros et al. (2011)
15.02.2011	X2.2	S20W12	170nm	AIA SDO	60	Maurya et al. (2012)
24.02.2011	M3.5	N14E 87	617.3nm	HMI SDO	15	Oliveros et al. (2012)
12.03.2012	M6.3	N15W01	360nm	ONSET China	25	Hao et al. (2012)
			425nm		12	

Conclusion

Spatially resolved observations with the SDO, TRACE and RHESSI show fine structure in flares. Flare plasma is confined in fine loop structures. HXR emission originates in lower chromosphere, SXR and EUV emissions are produced in high chromosphere, transition region and low corona. The processes causing WLFs are not sufficiently clear and the height of their origin is argued. Spatially and temporally correlated WL and HXR emissions show that continuum enhancement and accelerated electrons are closely related. A well-defined model, which would be able to explain WLF producing above the solar photosphere, is need.

Acknowledgements

References

Battaglia, M. and Kontar, E. P.: 2011a, Astrophys. J. 735, 42, doi: 10.1088/0004-637X/735/1/42.

Battaglia, M. and Kontar, E. P.: 2011b, Astron. Astrophys. 533, L2, doi: 10.1051/0004-361/201117605.

Cheng, X., Zhang, J., Liu, Y., Ding, M. D.: 2011, Astrophys. J. Lett. 732, L25, doi: 10.1088/2041-8205/732/2/L25

Delone, A. B., Yakunina, G. V., Porfir'eva G. A.: 2003, Izvestya RAN, ser. Phys. 67, N 3, 387.

Doschek, G. A., Strong, K.T., Tsuneta, S.: 1995, Astrophys. J. 440, 370, doi: 10.1086/175279.

Ding, M. D.: 2007, in P. Heinzel, I. Dorotovic and R. J. Rutten (ed.) ASP Conf. Ser., 368, 417.

Fletcher, L., Hannah, I. G., Hudson, H. S., and Metcalf, T. R.: 2007, Astrophys. J. 656, 1187, doi: 10.1086/510446.

Hao, Q., Guo, Y., Dai, Y., et al.: 2012, Astron. Astrophys. 544, L17, doi: 10.1051/0004-361/201219941.

Hudson, H. S., Wolfson, C. J., and Metcalf, T. R.: 2006, Solar Phys. 234, 79, doi: 10.1007/s11207-006-0056-y.

Jess, D. B., Mathioudakis, M., Crockett, P. J., and Keenan, F. P.: 2008, Astrophys. J. 688, L119, doi: 10.1086/595588.

Jing, J., Chae, J., and Wang, H.: 2008, Astrophys. J. 672, L72, doi: 10.1086/526339.

Kontar, E. P., Hannah, I. G., Jeffrey, N. L. S., and Battaglia M.: 2010, Astrophys. J. 717, 250, doi: 10.1088/0004-637X/717/1/250.

Kretzschmar, M.: 2011, Astron. Astrophys. 530, A84, doi:10.1051/0004-6361/201015930.

Krucker, S., Hudson, H. S., Jeffrey, N. L. S. et al.: 2011, Astrophys. J. 739, 96, doi: 10.1088/0004-637X/739/2/96.

Lemen, J. R., Title, A. M., Akin, D. J. et al. : 2012, Solar Phys, 275, 17, doi: 10.1007/s11207-011-9776-8.

Liu,Y., Ding, M. D., Fang, C.: 2001, Astrophys. J. 563, L169, doi: 10.1086/338734.

Maurya, R. A., Vemareddy, P., and Ambastha, A.: 2012, Astrophys. J. 747, 134, doi: 10.1088/0004-637X/747/2/134.

Oliveros, J.-C. M., Couvidat, S., Shou, J. et al.: 2011, Solar Phys. 269, 269, doi: 10.1007/s11207-010-9696-z.

Oliveros, J.-C. M., Hudson, H. S., Hurford, G. J. et al.: 2012, Astrophys. J. Letters. 753, L26, doi: 10.1088/2041-8205/753/2/L26.

Raymond, J. C., Krucker, S., Lin, R. P., Petrosian,V.: 2012, Space Sci. Rev. 173, 197, doi: 10. 1007/s11214-012-9897-x.

Reeves, K. K., and Golub, L.: 2011, Astrophys. J. 727, L52, doi: 10.1088/2041-8205/727/2/L52.

Veronig, A. M., and Brown J. C.: 2004, Astrophys. J. 603, L117, doi: 10.1086/383199.

Wang, H.-M.: 2009, Res. Astron. Astrophys. 9, 127, doi: 10.1088/1674-4527/9/2/001.

Watanabe, K., Krucker, S., Hudson, H. et al.: 2010, Astrophys. J. 715, 651, doi: 10.1088/0004-637X/715/1/651.

Warren, H. P. : 2000, Astrophys. J. 536, L105. doi: 10.1086/312734.

White, S. M., Benz, A. O., Christe, S. et al.: 2011, Space Sci. Rev. 159, 225, doi: 10.1007/s11214-010-9708-1.

Xu, Y., Cao, W., Liu, C. et al.: 2004, Astrophys. J. 607, L131, doi:10.1086/422099.

Xu, Y., Cao, W., Liu, C. et al.: 2006, Astrophys. J. 641, 1210, doi: 10.1086/500632.